

REGULAR PAPER

Effect of radiation-induced heat transfer on the temperature measurements in externally heated diamond anvil cells

To cite this article: Caihong Jia *et al* 2021 *Jpn. J. Appl. Phys.* **60** 106501

View the [article online](#) for updates and enhancements.



Effect of radiation-induced heat transfer on the temperature measurements in externally heated diamond anvil cells

Caihong Jia¹, Yang Gao^{2*}, Tingting Ji¹, Dawei Jiang¹, Min Cao¹, and Chunxiao Gao^{1*}

HPSTAR
1250-2021

¹State Key Laboratory of Superhard Materials, Jilin University, Changchun 130012, People's Republic of China

²Center for High Pressure Science and Technology Advanced Research, Beijing 10094, People's Republic of China

*E-mail: gysaong@hotmail.com; cc060109@qq.com

Received May 24, 2021; revised August 2, 2021; accepted August 25, 2021; published online September 7, 2021

The study of the thermal transport property of matter under extreme conditions is a significant but challenging task in the science community due to the unsatisfactory accuracy of heat flow characterization experimentally. In this work, a radiative-conductive coupled heat transfer model was proposed to resolve the heat transfer process inside a diamond anvil cell (DAC) under static heating conditions. The rationality of the model was verified via the characterization of the thermal conductivity of type Ia diamond. It is found that obvious error can come from the measurement of temperature by thermocouples in DAC. Based on this model, a temperature correction method with certain universality is presented for accurate temperature measurement by thermocouples in high-temperature experiments. The construction of the proposed model combined with the new correction method for temperature measurements may provide an efficient method for measuring potential thermal conductivity in a Bassett-type externally heated DAC. © 2021 The Japan Society of Applied Physics

Supplementary material for this article is available [online](#)

1. Introduction

The study of thermal transport properties of rocks and minerals under extreme conditions, such as high pressure and temperature (HP-HT), can provide valuable insights into the physical, chemical properties, mantle core characteristics, and dynamic processes of minerals in the Earth.^{1–6)} The development of these studies is crucial in mantle mineralogy, geophysics, and chemistry.^{7–11)} Diamond anvil cells (DACs), the most common experimental apparatus used to provide a direct simulation of the HP-HT environment in the Earth's interior, have attracted the keen interest of researchers in these areas.^{12–17)} However, difficulties such as the accurate characterization of the samples' heat flow field remain when DACs are utilized as the measurement platform.¹⁸⁾ Accurate description of the temperature distribution within the DAC is essential for the characterization of the samples' heat flow field.^{19–21)} Besides, the heat transfer mode in an externally heated DAC is quite complicated. Heat flows through the sample and dissipates into the environment via convection, including radiation at the same time. Heat convection can be effectively eliminated by obliterating the medium, air around the system.²²⁾ However, heat radiation must be considered in both experiments and theoretical calculations.

The impact of radiation on the measurement of thermo-physical properties is in-negligible at high temperatures.^{23–25)} Besides development in experimental methods, computer-aided methods such as computational fluid dynamics (CFD) has been proved to be an accurate tool for these investigations in cases such as flame radiation, surface radiation heat transfer, convection, and radiation coupled heat transfer in the process with or without participating media. In particular, the finite volume method (FVM), one of the main branches in CFD, has been utilized in most cases and generated promising results.^{26–29)} Amirjavad et al.²⁶⁾ used FVM to numerically analyze the radiant heat flow distribution of the methane-air diffusion flame. Venkatadri et al.²⁷⁾ studied the influence of heat radiation on natural convection inside the trapezoidal enclosure using FVM. Shirvan et al.²⁸⁾ found that the coupled heat transfer between radiation and natural

convection could be maximized by increasing the wall emissivity and Rayleigh number in a parabolic solar cavity receiver. Fu et al.²⁹⁾ used FVM numerical analysis to analyze the heat transfer mechanism of the interaction between natural convection and surface radiation during the heating process in the resistance furnace.

However, most investigations of the coupled conduction with radiation heat transfer have focused on systems in one or two-dimensional spaces, which, in most cases, are not sufficient in a system as complicated as the heated DAC. The conduction, as well as the transmission and absorption of radiation in the three-dimensional (3D) space, have to be considered in this case.³⁰⁾ Currently, very few researches on nonlinear 3D radiation heat transfer models have been reported.

In this paper, a 3D model was proposed for heat transfer simulation based on the “Bassett type” externally heated DAC, which heats the diamond seats, under vacuum conditions.¹²⁾ Specifically, we have performed the characterization of type Ia diamonds' heat transfer properties both experimentally and theoretically. Experimentally, the utilization of a self-designed water-cooled DAC in vacuum has provided us the expected heat flow environment without heat convection.¹⁹⁾ Theoretically, we proposed a coupled radiative-conductive heat transfer numerical model for the heat transfer behavior of diamonds to demonstrate the complicated heat transfer modes in a Bassett-type externally heated DAC. The theoretical results were then compared with the experimental data to verify the rationality of the model. A temperature correction method based on this model was then proposed for a Bassett-type externally heated DAC in which the thermocouples were utilized as temperature calibrators.

2. Mathematical model

The proposed mathematical model was developed based on FVM. The simulation of the heat transfer mechanism of the diamond anvils and gasket in the DAC was carried out by nonlinear surface radiation-conduction coupling (NSRC) and nonlinear 3D radiation-conduction coupling (NTRC) heat transfer mode.

A few preconditions and assumptions are drawn in the simulation:

- i) In the experiment, the surrounding environment of a Bassett-type externally heated DAC was first vacuumed ($<10^0$ Pa) to minimize the effects of natural convection before heating. Therefore, the environment in the simulation is set to vacuum according to the experiment.
- ii) The effects of natural heat convection around the DAC were minimized in the experiment; thus, the temperature distribution in the DAC is governed by heat conduction and radiation in the simulation.
- iii) In the experiment, the temperature of the anvils' back surfaces was carefully monitored and controlled at certain values to maintain static heating conditions within the DAC. Therefore, the temperature of the anvils' back surfaces is considered constant in the simulation.
- iv) The radiation characteristics of diamonds vary with wavelength. In this simulation, the radiation spectrum of diamonds is divided into eight independent bands with wavelengths 200–470; 470–580; 580–2500; 2500–3703; 3703–6667; 6667–9550; 9550–10848; 10848–50000 nm, respectively.

2.1. Model description

The simulation model (Fig. 1) consists of two main components: diamond anvils and gasket (DG). Before the experiment, a spectrophotometer (Shimadzu UV-3600) was used to measure the infrared spectroscopy spectra of diamond anvil [Fig. S1 (available online at stacks.iop.org/JJAP/60/106501/mmedia) in the supporting information]. Based on the spectra obtained from infrared spectroscopy and experimental equation,^{31,32} the nitrogen concentration is 1710 ppm. The

type Ia diamond anvils are mounted on the seats heated according to the “Bassett type” externally heating method by a resistance furnace. Once the seat is heated, the simulation establishes two heat transfer pathways: heat conduction or radiation-conduction coupling from the anvils to the spacer and radiation energy consumption (REC) via surface radiation between the environment and the DAC. The equations characterizing these two pathways are as follows:

$$\frac{\partial}{\partial t}(\rho E) + \frac{\partial}{\partial x_i}(u_i(\rho E + p)) = \frac{\partial}{\partial x_i} \left(k_{\text{eff}} \frac{\partial T}{\partial x_i} - \sum_j h_j \vec{J}_j + u_i(\tau_{ij})_{\text{eff}} \right) + S_h, \quad (1)$$

where ρ , k_{eff} , \vec{J}_j , E , h_j , and S_h are mass density, effective thermal conductivity in W/(m · K), the setting of motion properties of the solid region, the diffusion flux of the component j , the energy per unit mass, the enthalpy, and the source item, including the heat generated by a volumetric source in the solid zone, respectively. The left-hand side of Eq. (1) is the pressure and kinetic energy terms, and the right-hand side is the energy transfer due to heat conduction, component diffusion, and viscous dissipation.

Unlike the general energy and heat transfer equations, the radiation transfer equation describes heat transfer along arbitrary directions in 3D space and thus the gradient terms are not included. Equation (1) of the coupled conduction and radiation heat transfer relates the radiation transfer equation and the heat conduction equation using the source term S_h . By considering absorption, emission, and scattering of the solid zone, the radiation transfer equation can be written as follows:

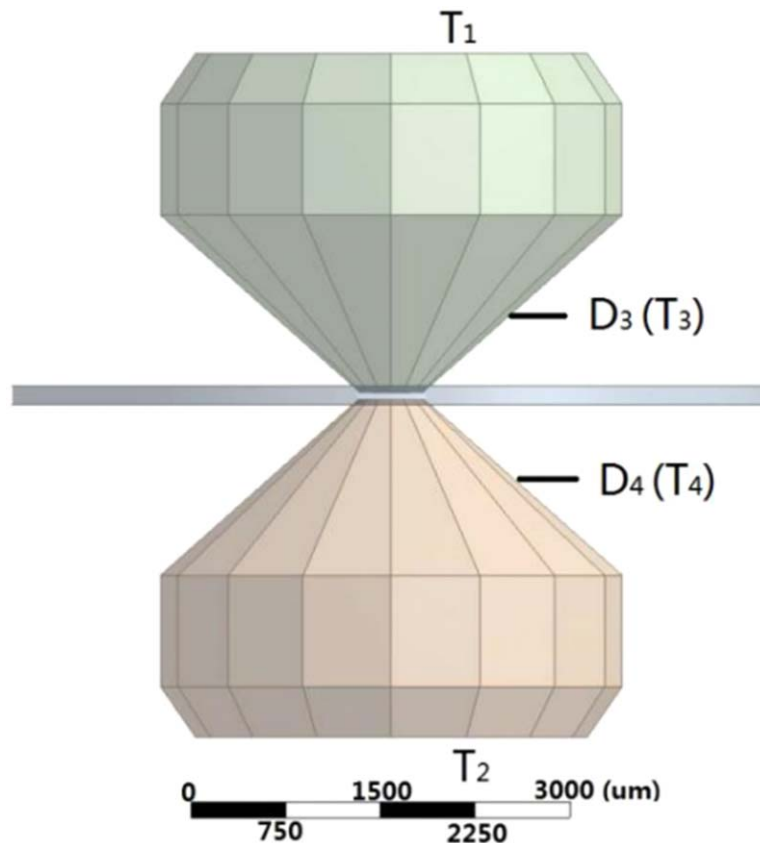


Fig. 1. (Color online) Schematics of the diamond anvils and gasket in the simulation.

$$\nabla \cdot [I_\lambda(\vec{r}, \vec{s}) \cdot \vec{s}] + (\alpha_\lambda + \sigma_s)I_\lambda(\vec{r}, \vec{s}) = \alpha_\lambda n^2 I_{b\lambda} + \frac{\sigma_s}{4\pi} \int_0^{4\pi} I_\lambda(\vec{r}, \vec{s}') \phi(\vec{s} \cdot \vec{s}') d\Omega', \quad (2)$$

where α_λ , σ_s , ϕ , Ω , λ , and $I_{b\lambda}$ are the absorption coefficient, the scattering coefficient, the phase function, solid angle, the radiation wavelength, and the blackbody radiation intensity, respectively.

2.2. Initial and boundary conditions

The initial condition for the simulation is the temperature of the anvils' back surfaces,

$$[T(x, y, z)]_{t=0} = T_1, [T(x, y, z)]_{t=0} = T_2, \quad (3)$$

where T_1 and T_2 are the temperature values of back surfaces of the top and bottom diamond anvils, respectively.

The quantity of the emergent radiation gives the boundary condition from the surface to the surrounding environment as follows:

$$q_{\text{net}} = \varepsilon\sigma(T_w^4 - T_e^4), \quad (4)$$

where q_{net} is the net radiation exchange, the total heat dissipation to the outer surface of the DAC; ε , T_w , and T_e are the emissivity, surface temperature of DG, and temperature of the surrounding environment.

3. Result and discussion

Based on the radiation-conduction coupling heat transfer model, the proposed mathematical model for the thermal conductivity of materials between two diamond anvils under static heating was developed. For comparison, two independent models using NSRC and NTRC modes were constructed for measurements. The type Ia diamond anvils, which have experimentally been measured and considered necessary reference materials in thermal measurements in a DAC, are selected as both the test object and the reference material. The radiation properties of type Ia diamonds were first characterized using a spectroscopic method to measure its thermal conductivity using the proposed model.

In order to verify the rationality of the proposed model, we compared the measurement results via the surface radiation-conduction coupling and 3D radiation-conduction coupling heat transfer model to those from the flash diffusivity method. Furthermore, a temperature correction method is proposed for thermocouples based on the radiation-conduction coupling heat transfer model, which could be used to calibrate the temperature acquired by thermocouples in vast high-temperature measurements.

3.1. Thermal radiation characteristics of the type Ia diamond

Diamond is a semi-transparent material whose radiation is inevitable during heat transfer processes.³³⁾ Therefore, the transmission and absorption of radiation inside the diamond have to be considered during the simulation. However, the optical parameters, including transmittance, reflectivity, and absorptivity of type Ia diamond in the thermal radiation band, have never been reported so far.

In this research, a spectrophotometer (Shimadzu UV-3600) was used to characterize the thermal radiation characteristics of the type Ia diamond anvils for the simulation. The optical parameters, including the reflection spectrum (Fig. S2),

transmittance spectra (Fig. S3), and absorption spectra (Fig. S4), are thus recorded. The optical constant emissivity ε , absorption coefficient α , and complex refractive index n can be calculated using the following expressions.³³⁾

$$T_\lambda = \frac{(1 - R_\lambda)^2 D}{1 - R_\lambda^2 D^2},$$

$$R_\lambda = \frac{(1 - n)^2 + k^2}{(1 + n)^2 + k^2},$$

$$D = \exp(-\alpha d), \alpha = 4\pi k\nu, \quad (5)$$

where d and ν denote the thickness and frequency of diamond; n and k represent the refractive indices. The absorption coefficient α , optical constant emissivity ε , and complex refractive index n of type Ia diamond are shown in Fig. 2. Table I presents the corresponding characteristics of type Ia diamonds.

3.2. Effects of radiative-conductive coupled heat transfer on the heat flow field in DAC

The FVM simulation of the system was performed to develop a mathematical model that best matches the actual physical processes inside the DAC. Different heat transfer pathways, such as NSRC and NTRC heat transfer, have been included in the simulation for comparison. Tables I and II show the thermal properties of the anvil and gasket associated with the numerical model.

In order to study the contribution of radiation heat transfer to the entire temperature field in DG, the radiation-conduction coupling heat transfer model is used in the simulation with different temperature boundaries T_1 and T_2 . The heat loss ratio caused by surface radiation and 3D radiation is then analyzed. In the simulation, T_1 was set at 483, 583, and 883 K, while T_2 was varied to simulate different conditions. The ratios of heat loss by surface radiation and 3D radiation are shown in Fig. 3, with the abscissa referring to the temperature difference between T_1 and T_2 (Table III in supporting information). Figure 3 shows a certain difference in REC generated by surface radiation and 3D radiation in the DAC under static heating. Under the same temperature

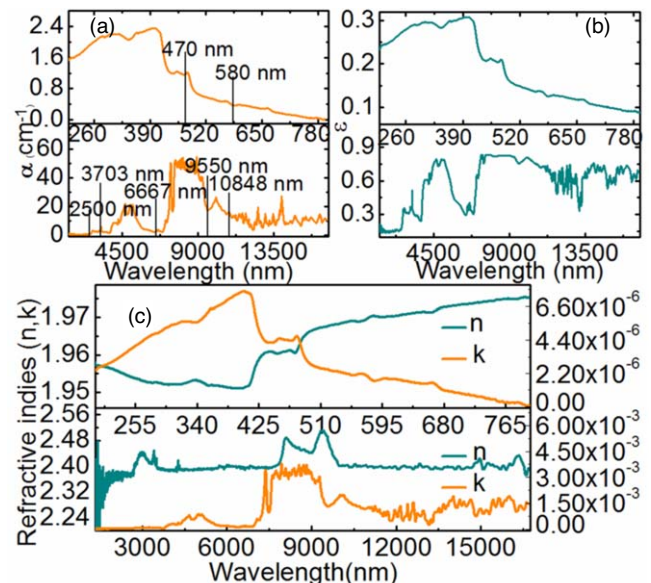


Fig. 2. (Color online) The (a) absorption coefficient, (b) emissivity, and (c) refractive indices of type Ia diamond.

Table I. Thermal radiation characteristics of type Ia diamond.

Band (nm)/Property	Emissivity	Absorption coefficient (cm ⁻¹)	Refractive index
200–470	0.28	1.83	1.95
470–580	0.15	0.56	1.96
580–2500	0.1	0.23	1.97
2500–3703	0.24	2.23	2.3
Band(nm)/prop-erty	Emissivity	Absorption coeffi-cient (cm ⁻¹)	Refractive index
3703–6667	0.55	14.68	2.4
6667–9550	0.6	46.67	2.4
9550–10848	0.65	19.77	2.45
10848–50000	0.57	12.73	2.4

Table II. Thermochemical parameters of materials used in model calculations.

Property/Material	Diamond	Spacer
Density (kg/m ³)	3520	7000
Thermal conductivity (W/(m · K))	Function of temperature ³⁴⁾	Function of temperature ³⁵⁾
Specific heat capacity (J/(kg · K))	Function of temperature ³⁵⁾	460

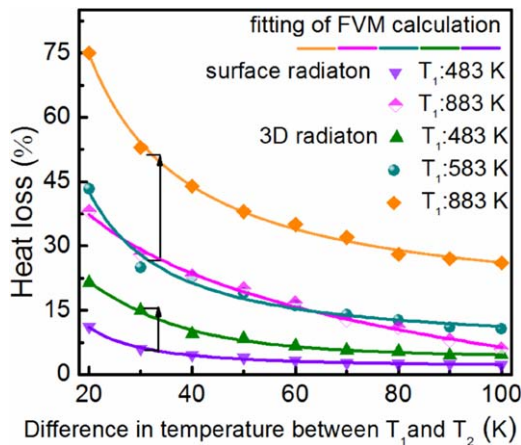


Fig. 3. (Color online) The ratio of heat loss caused by radiation-conduction coupling heat transfer.

boundary conditions T_1 and T_2 , the REC caused by 3D radiation is greater than that caused by surface radiation. As shown in Fig. 3, increasing the temperature difference reduces radiation loss, indicating that the REC can be reduced by adjusting the temperature boundary conditions.

3.3. Validation of the radiation-conduction coupling heat transfer model

In order to verify the rationality of the proposed model, we compared our simulated thermal conductivity of type Ia diamond with that obtained through the experiment. Based on the temperature measurements via thermocouples,³⁴⁾ the simulation of thermal conductivity of type Ia diamond was performed using NSRC and NTRC heat transfer models. In this scheme, T_1 (T_2) is the top (bottom) anvil’s back surface temperature and T_3 (T_4) is the temperature at the midpoint D_3 (D_4) of the top (bottom) anvil lateral edges. The T_1 and T_2 are used as temperature boundary conditions in the simulation. In all simulations, it is assumed that the thermal conductivity of the type Ia diamond changes until the calculated temperatures t_3' and t_4' at the midpoints D_3 and D_4 reach the measured

temperatures T_3 and T_4 . Thus, the input thermal conductivity is matched by the real type Ia diamond thermal conductivity. Figure S5 presents the flow block diagram for calculating the thermal conductivity of type Ia diamond in the supporting information.

As demonstrated in Fig. 4, the thermal conductivity of diamond obtained from both models is comparable to that obtained from Yue et al.’s³⁴⁾ results and the Olson et al.’s³⁶⁾ results using the flash diffusivity method, yet shows minimal deviation from each other. The simulation results using the surface radiation model yield almost the same thermal conductivity as that from Yue et al.’s results by heat conduction model.³⁴⁾ Hence, it is clear that the heat loss caused by surface radiation is minimal and shows limited effects on diamonds’ thermal conductivity at temperatures between 320 and 570 K. This is consistent with the radiant heat loss ratio obtained in the previous part. However, the result from the NTRC heat transfer model is more conformable with Olson et al.’s data as the diamond anvils temperature increases.³⁶⁾ Given the significant radiation effect at high temperatures and thermal radiation characteristics of the diamond anvil, the NTRC heat transfer model is the most consistent with the actual physical process of DG at high temperatures.

3.4. Effect of radiant heat transfer on the accuracy of thermocouples

Figure 1 shows that when the temperature boundary conditions are fixed, the thermal conductivity of materials can be obtained by simulating temperature at the midpoint D_3 and D_4 of the diamond anvils lateral edges using the NTRC heat transfer model. In experiments, the measured accuracy of T_3 and T_4 are primarily affected by heat radiation. Here, we used the proposed model to get the temperature correction value for the thermocouple readings T_3 and T_4 to accurately simulate the whole system, corrections on T_3 and T_4 values are required.

We used FVM to analyze the specific value of thermocouple temperature calibration quantitatively and calibrated the error caused by the radiation effect at the same time. Figure 5 shows that the temperature correction values of T_3

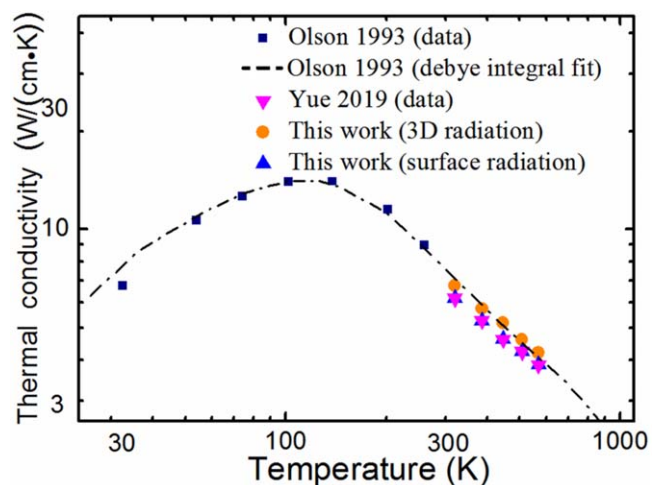


Fig. 4. (Color online) The thermal conductivity of type Ia diamond: The data of Olson³⁴⁾ is shown with squares (navy). The Debye integral fitting function of Olson³⁴⁾ is shown with dash-dot (black). The data of Yue³²⁾ is shown with triangles (magenta). The data of this work is shown with circles (green) and triangles (blue).

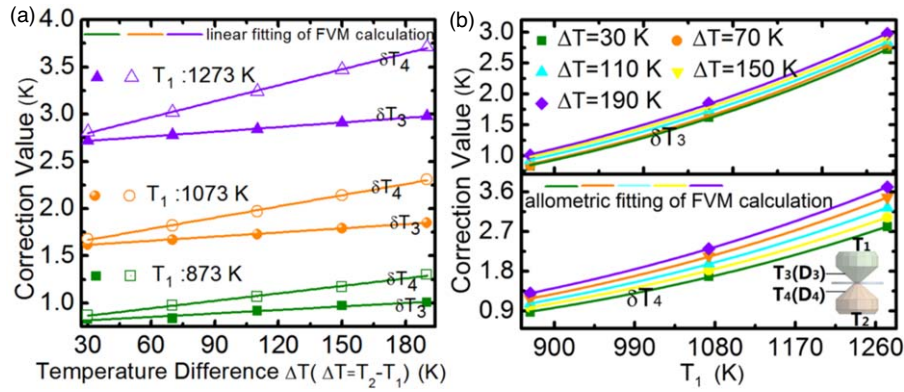


Fig. 5. (Color online) D_3 and D_4 thermocouple calibration data, δT_3 is the temperature correction value of the upper diamond lateral edge (at the midpoint D_3), δT_4 is the temperature correction value of the lower diamond lateral edge (at the midpoint D_4).

and T_4 (δT_3 and δT_4) as a power function of T_1 and a linear function of temperature difference ΔT ($\Delta T = T_2 - T_1$). Both δT_3 and δT_4 increase with the increase in temperature difference ΔT , as shown in Fig. 5(a). Figure 5(b) depicts the temperatures correction value of T_3 and T_4 , which increases with the elevation of T_1 when the temperature difference ΔT is constant. With the elevation in temperatures T_1 and T_2 , the correction value of both T_3 and T_4 increases accordingly, showing that the measurement accuracy of thermocouples deteriorates with temperature elevation. Thus, corrections on the temperature yielded from the thermocouples are needed to better characterize the thermal conductivity properties of materials at high temperatures. Based on the above analysis, the general expression of the temperatures correction is obtained as follows:

$$\delta T_{3/4} = aT_1^b + c(T_2 - T_1) + d. \quad (6)$$

The δT_3 and δT_4 can be expressed as:

$$\delta T_3 = 0.0019(T_1 - 273.15)^{1.1081} + 0.001(T_2 - T_1) - 1.4078 \quad (7)$$

$$\delta T_4 = 0.0027(T_1 - 273.15)^{1.0375} + 0.002(T_2 - T_1) - 0.8574. \quad (8)$$

The result of FVM calculation and analysis indicates that the correction method is reasonable and could be widely utilized in a Bassett-type externally heated DAC that uses thermocouples as temperature calibrate. The use of temperature correction in high-temperature experiments will enhance the accuracy of thermal measurements under extreme conditions.

4. Conclusions

A 3D radiation-conduction coupled model for thermal conductivity measurements in a DAC under static heating was developed using FVM. Compared with the previous models, the proposed model measures heat radiation that participates in diamond anvil's heat transfer and REC generated by the surface DG into the simulation. The result shows that the contribution of the radiation effect to the entire temperature field cannot be neglected. Based on simulation results, the radiation effect under static heating demonstrates an increasing trend with the temperature's rise of diamond anvil's back surfaces. Comparison between the proposed nonlinear

3D radiation-conduction coupling heat transfer model and the previous model shows that radiation effects play a non-ignorable role in the precise characterization of materials' thermal conductivity in a DAC under static heating. Correction on the temperature yielded from the thermocouples is necessary for thermal conductivity measurements and high temperature-related measurements in a DAC. A temperature correction method with certain universality is established based on this model. The proposed model serves as a more practical and accurate temperature measurement method for the high-temperature investigations in a Bassett-type externally heated DAC.

Acknowledgments

This work is supported by the National Key Research and Development Program of China (No. 2018YFA0702700) and the National Natural Science Foundation of China (Grant Nos. 11674404, 11774126).

- 1) M. W. Ammann, A. M. Walker, S. Stackhouse, J. Wookey, A. M. Forte, J. P. Brodholt, and D. P. Dobson, *Earth Planet. Sci. Lett.* **390**, 175 (2014).
- 2) S. S. Lobanov, N. Holtgrewe, and A. F. Goncharov, *Earth Planet. Sci. Lett.* **449**, 20 (2016).
- 3) N. Koker, *Earth Planet. Sci. Lett.* **292**, 392 (2010).
- 4) D. A. Dalton, W. P. Hsieh, G. T. Hohensee, D. G. Cahill, and A. F. Goncharov, *Sci. Rep.* **3**, 2400 (2013).
- 5) H. Vosteen and R. Schellschmidt, *Phys. Chem. Earth* **28**, 499 (2003).
- 6) Y. Okuda, K. Ohta, A. Hasegawa, T. Yagi, K. Hirose, S. I. Kawaguchi, and Y. Ohishi, *Earth Planet. Sci. Lett.* **547**, 116466 (2020).
- 7) C. Wang, A. Yoneda, M. Osako, E. Ito, T. Yoshino, and Z. M. Jin, *J. Geophys. Res. Solid Earth* **119**, 6277 (2014).
- 8) F. C. Marton, T. J. Shankland, and D. C. Rubie, *Phys. Earth Planet. Inter.* **149**, 53 (2005).
- 9) F. D. Stacey and D. E. Loper, *Phys. Earth Planet. Inter.* **161**, 13 (2007).
- 10) T. K. B. Tomohiko, M. Nakada, and D. A. Yuen, *Earth Planets Space* **57**, 15 (2005).
- 11) Z. H. Sun, K. P. Yuan, X. L. Zhang, and D. W. Tang, *Phys. Chem. Chem. Phys.* **20**, 30331 (2018).
- 12) W. A. Bassett, A. H. Shen, M. Bucknum, and I. M. Chou, *Rev. Sci. Instrum.* **64**, 2340 (1993).
- 13) J. Yan, A. Doran, A. A. MacDowell, and B. Kalkan, *Rev. Sci. Instrum.* **92**, 013903 (2021).
- 14) M. Louvel, J. W. E. Drewitt, A. Ross, R. Thwaites, B. J. Heinen, D. S. Keeble, C. M. Beavers, M. J. Walterd, and S. Anzellini, *J. Synchrotron Radiat.* **27**, 529 (2020).
- 15) Y. Okuda, S. Kimura, K. Ohta, Y. Park, T. Wakamatsu, I. Mashino, and K. Hirose, *Rev. Sci. Instrum.* **92**, 015119 (2021).
- 16) Z. X. Du, L. Miyagi, G. Amulele, and K. K. M. Lee, *Rev. Sci. Instrum.* **84**, 024502 (2013).
- 17) K. Shinoda and N. Noguchi, *Rev. Sci. Instrum.* **79**, 015101 (2008).

- 18) G. I. Pangilinan, H. D. Ladouceur, and T. P. Russell, *Rev. Sci. Instrum.* **71**, 3846 (2000).
- 19) D. H. Yue, T. T. Ji, T. R. Qin, J. Wang, C. L. Liu, H. Jiao, L. Zhao, Y. H. Han, and C. X. Gao, *Appl. Phys. Lett.* **112**, 081901 (2018).
- 20) D. A. Polvani, Y. Fei, J. F. Meng, and J. V. Badding, *Rev. Sci. Instrum.* **71**, 3138 (2000).
- 21) D. A. Polvani, J. F. Meng, M. Hasegawa, and J. V. Badding, *Rev. Sci. Instrum.* **70**, 3586 (1999).
- 22) S. Pasternak, G. Aquilanti, S. Pascarelli, R. Poloni, B. Canny, M. V. Coulet, and L. Zhang, *Rev. Sci. Instrum.* **79**, 085103 (2008).
- 23) R. Coquard, J. Randrianalisoa, S. Lallich, and D. Baillis, *J. Heat Transfer* **133**, 112604 (2011).
- 24) S. Wang, Q. Ai, T. Q. Zou, C. Sun, and M. Xie, *Appl. Therm. Eng.* **177**, 32574 (2020).
- 25) U. Gross and L. Tran., *Int. J. Heat Mass Transfer* **47**, 3279 (2004).
- 26) A. A. Hosseini, M. Ghodrat, M. Moghiman, and S. H. Pourhoseini., *Case Stud. Therm. Eng.* **18**, 100610 (2020).
- 27) K. Venkatadri, O. A. Bégb, P. Rajarajeswari, and V. R. Prasad., *Int. J. Mech. Sci.* **171**, 105391 (2020).
- 28) K. M. Shirvan, M. Mamourian, S. Mirzakanlari, A. B. Rahimi, and R. Ellahi, *Int. J. Numer. Methods Heat Fluid Flow* **27**, 2385 (2017).
- 29) Z. L. Fu, X. H. Yu, H. L. Shang, Z. Z. Wang, and Z. Y. Zhang., *Int. J. Heat Mass Transfer* **128**, 679 (2019).
- 30) H. Zhang, Y. M. Li, and W. Q. Tao, *Appl. Therm. Eng.* **114**, 337 (2017).
- 31) C. Fang, X. P. Jia, N. Chen, Y. D. Li, L. S. Guo, L. C. Chen, H. Ma, and X. B. Liu, *J. Cryst. Growth* **436**, 34 (2016).
- 32) M. H. Hu, N. Bi, S. S. Li, T. C. Su, Q. Hu, H. Ma, and X. P. Jia, *CrystEngComm* **19**, 4571 (2017).
- 33) P. Dore et al., *Appl. Opt.* **37**, 5731 (1998).
- 34) D. H. Yue, Y. Gao, L. Zhao, Y. L. Yan, T. T. Ji, Y. H. Han, and C. X. Gao, *Jpn. J. Appl. Phys.* **58**, 040906 (2019).
- 35) M. Zainulabdein, H. Ijaz, and W. Saleem., *Materials* **10**, 739 (2017).
- 36) J. R. Olson, R. O. Pohl, J. W. Vandersande, A. Zoltan, T. R. Anthony, and W. F. Banholzer, *Phys. Rev. B* **47**, 14850 (1993).